



## RESEARCH ARTICLE

# Mapping Unsaturation in Human Plasma Lipids by Data-Independent Ozone-Induced Dissociation

David L. Marshall,<sup>1</sup> Angela Criscuolo,<sup>2,3,4</sup> Reuben S. E. Young,<sup>5</sup> Berwyck L. J. Poad,<sup>1</sup> Martin Zeller,<sup>4</sup> Gavin E. Reid,<sup>6</sup> Todd W. Mitchell,<sup>7,8</sup> Stephen J. Blanksby<sup>1</sup>

<sup>1</sup>Central Analytical Research Facility, Institute for Future Environments, Queensland University of Technology, Brisbane, QLD 4000, Australia

<sup>2</sup>Institute of Bioanalytical Chemistry, Faculty of Chemistry and Mineralogy, Universität Leipzig, Leipzig, Germany

<sup>3</sup>Center for Biotechnology and Biomedicine, Universität Leipzig, Leipzig, Germany

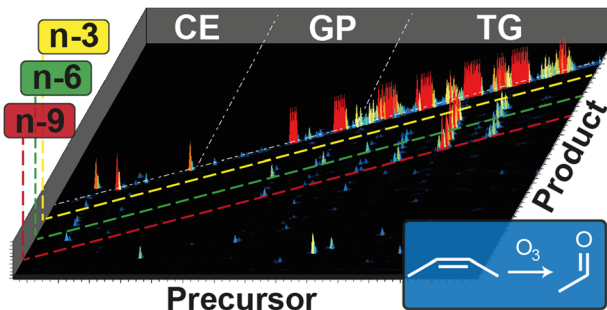
<sup>4</sup>Thermo Fisher Scientific (Bremen) GmbH, Hanna-Kunath Str. 11, 28199, Bremen, Germany

<sup>5</sup>School of Chemistry, Physics and Mechanical Engineering, Queensland University of Technology, Brisbane, Australia

<sup>6</sup>School of Chemistry, Department of Biochemistry and Molecular Biology, Bio21 Molecular Science and Biotechnology Institute, The University of Melbourne, Parkville, Australia

<sup>7</sup>School of Medicine and Molecular Horizons, University of Wollongong, Wollongong, Australia

<sup>8</sup>Illawarra Health and Medical Research Institute, Wollongong, Australia



**Abstract.** Over 1500 different lipids have been reported in human plasma at the sum composition level. Yet the number of unique lipids present is surely higher, once isomeric contributions from double bond location(s) and fatty acyl regiochemistry are considered. In order to resolve this ambiguity, herein, we describe the incorporation of ozone-induced dissociation (OzID) into data-independent shotgun lipidomics workflows on a high-resolution hybrid quadrupole-Orbitrap

platform. In this configuration,  $[M + Na]^+$  ions generated by electrospray ionization of a plasma lipid extract were transmitted through the quadrupole in 1 Da segments. Reaction of mass-selected lipid ions with ozone in the octopole collision cell yielded diagnostic ions for each double bond position. The increased ozone concentration in this region significantly improved ozonolysis efficiency compared with prior implementations on linear ion-trap devices. This advancement translates into increased lipidome coverage and improvements in duty cycle for data-independent MS/MS analysis using shotgun workflows. Grouping all precursor ions with a common OzID neutral loss enables straightforward classification of the lipidome by unsaturation position (with respect to the methyl terminus). Two-dimensional maps obtained from this analysis provide a powerful visualization of structurally related lipids and lipid isomer families within plasma. Global profiling of lipid unsaturation in plasma extracts reveals that most unsaturated lipids are present as isomeric mixtures. These new insights provide a unique picture of underlying metabolism that could in the future provide novel indicators of health and disease.

**Keywords:** Lipidomics, Ozone-induced dissociation, Data-independent analysis, Plasma

Received: 1 April 2019/Revised: 27 May 2019/Accepted: 27 May 2019/Published Online: 20 June 2019

**Electronic supplementary material** The online version of this article (<https://doi.org/10.1007/s13361-019-02261-z>) contains supplementary material, which is available to authorized users.

**Correspondence to:** David Marshall; e-mail: d20\_marshall@qut.edu.au, Stephen Blanksby; e-mail: stephen.blanksby@qut.edu.au

## Introduction

Human blood plasma is a tightly regulated biological fluid, rich in lipids and metabolites that is readily available in clinical settings. The composition of the plasma lipidome can provide a snapshot of human metabolism [1]. Moreover,

changes in plasma lipid concentrations have been widely studied in biomarker discovery for various pathologies, including Alzheimer's disease [2], prostate cancer [3], metabolic dysfunction [4], and cardiovascular disease [5], among others [6].

The unparalleled sensitivity and specificity of contemporary mass spectrometers (and associated developments in bioinformatics) have led to mass spectrometry-based methods becoming the analytical tool of choice for characterizing complex lipid extracts from biological systems; including human blood plasma. Plasma lipid extracts have been analyzed by high-resolution "top-down" shotgun lipidomics [7, 8], or in conjunction with prior fractionation by chromatographic and/or ion-mobility separations to resolve lipid classes [9–11], or unique lipids within a class [12]. These collective efforts have driven the development of certified standard reference materials (e.g., SRM1950: metabolites in human plasma, National Institute of Standards and Technology) [13] and isotopically labeled lipid standard mixtures (e.g., SPLASH® Lipidomix®, Avanti Polar Lipids) that mimic human plasma, to facilitate more accurate quantitation of plasma lipids. Despite these achievements, the challenge of fully elucidating the human plasma lipidome has been clearly laid out by an inter-laboratory study using SRM1950 [14]. Among the 1527 different lipids identified at the sum composition level (number of carbons and degree of unsaturation), consensus between 5 or more laboratories could only be reached for the concentration of 339 lipid species. Unsurprisingly, there is a continued impetus to develop guidelines in order to standardize lipidomics approaches in order to bridge the gap between the analytical laboratory and clinical diagnostics [15–17].

Yet even this startling result does not capture the full extent of the task confronting the lipidomics community. Assigning a lipid only at the sum composition level overlooks more detailed descriptions of molecular structure, referred to by Koelmel and co-workers as the structural resolution in lipid identification [18]. The inability to resolve isomeric species leads to a significant underestimation of the diversity of unique molecular species within the lipidome [19, 20], and raises the possibility that identified biomarkers are not unique molecules but instead represent a mixture of isomers. Isomeric overlap can arise in glycerolipids and glycerophospholipids from the presence of multiple species with a common lipid class and sum composition but varying in the composition and relative position (*sn*-position) of fatty acyl chains on the glycerol backbone. While acyl chain composition can be determined by tandem mass spectrometry (e.g., PC 16:0\_20:1 is resolved from PC 18:0\_18:1), regioisomers differing only in the position of the chains (e.g., PC 16:0/20:1 and PC 20:1/16:0) are typically resolved by exhaustive chromatographic or ion-mobility separations [21–23], combinations of CID with ion-molecule reactions [24, 25], or carefully calibrated CID-based methods [26–29]. Zacek and co-workers used a negative ion MS/MS-based approach to quantify isomeric phosphatidylcholines (PCs) in human plasma [30]. This analysis extended the list of 22 PCs identified by sum composition (e.g., PC 36:1) to 41 species with defined composition of the constituent fatty acids.

Moreover, both possible regioisomers were found to be present in 35 of these 41 PCs. Taken together, these data contribute an almost fourfold increase in the number of PCs assigned in human plasma (see Fig. 1). Although this regioisomer-specific analysis was conducted only on PCs, it is not difficult to envisage that such diversity would be replicated across all glycerolipid and glycerophospholipid classes.

The critical structural detail that remains beyond the reach of conventional MS/MS-based lipidomics is the assignment of double bond position and stereochemistry within a fatty acyl chain, which would complete the description of the "structurally defined molecular lipid" [31]. Double bond position has a significant impact on the physical properties of macromolecular lipid assemblies [32–34]. Moreover, changes in unsaturation position within the cellular lipidome (due to dysregulation of desaturase enzymes) have been implicated in various pathologies including cancer [35, 36]. However, double bond-specific fragmentation is typically not observed with low-energy CID, or the diagnostic ions are present only in minor abundance in complex spectra [37]. Resolution of lipid isomers varying only by double bond position has been successfully demonstrated by ion-mobility spectrometry [38–40], the Paternò-Büchi reaction [41], UV photodissociation [42, 43], electron impact excitation of ions from organics [44], or by chemical derivatization prior to tandem mass spectrometry analysis [45]. While some attempts have been made to apply these techniques to profiling unsaturation in free fatty acids from human plasma [46, 47], only recently has attention turned to unsaturation within complex plasma lipids [48]. Ozone-induced dissociation (OzID) exploits the chemical reaction between ozone and mass-selected lipid ions, thereby generating product ions with predictable neutral losses depending on the position(s) of unsaturation. [49, 50] In this work, OzID is implemented on a high-resolution hybrid quadrupole-Orbitrap mass spectrometer (Q Exactive™ HF) in order to profile unsaturation in multiple complex lipid classes extracted from

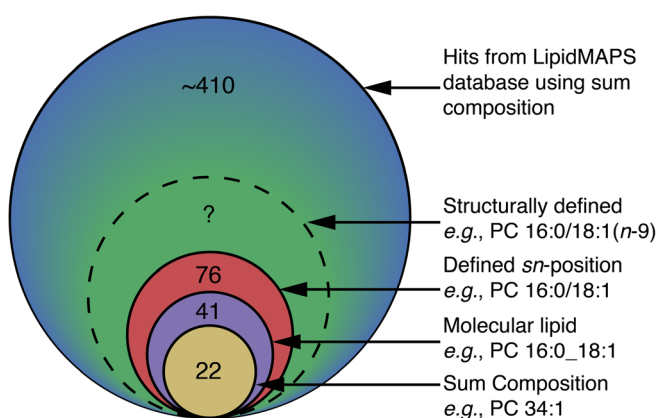


**Figure 1.** Hierarchical description of the number of unique PC lipids in human plasma. Experimental data taken from Zacek et al [30]. The outer circle is a theoretical maximum gained from searching the 22 reported PC sum compositions against the Lipid MAPS database

human plasma using a data-independent shotgun lipidomics approach.

## Experimental

### Materials

Optima LC-MS grade water, methanol, and HPLC grade methyl *tert*-butyl ether (MTBE) were obtained from Fisher Scientific (Schwerte, Germany) and used as received. Sodium acetate (LC-MS grade) and citrated human blood plasma were purchased from Sigma-Aldrich (Munich, Germany).

### Lipid Extraction and Sample Preparation

Lipids were extracted from 40  $\mu\text{L}$  aliquots of human plasma following an MTBE-based lipid extraction protocol, as previously described [51]. MTBE extracts were evaporated to dryness and subsequently re-dissolved in 800  $\mu\text{L}$  methanol containing 0.1 mM sodium acetate, as  $[\text{M} + \text{Na}]^+$  ions yield more abundant OzID product ions relative to  $[\text{M} + \text{H}]^+$  or  $[\text{M} + \text{NH}_4]^+$  precursor ions [38].

### Mass Spectrometry

Mass spectra were acquired in positive ion mode using a heated electrospray ionization source on a high-resolution Q Exactive™ HF hybrid quadrupole-Orbitrap mass spectrometer (Thermo Fisher Scientific, Bremen, Germany). The instrument was modified as shown in Supporting Information Fig. S1 to facilitate the introduction of ozone into the collision cell normally filled with nitrogen for higher-energy collisional dissociation (HCD). [52] As shown in Supporting Information Fig. S2, this configuration affords a significant increase in OzID product ion abundances compared with implementation in a linear ion-trap. Ozone (ca. 13% w/w  $\text{O}_2$ ) was produced online by an ozone generator (HC-30, Ozone Solutions, Hull, IA) and connected to a stainless-steel union tee with ozone-resistant 1/4" Teflon tubing. The ozone was supplied to the instrument via a PEEKsil™ restrictor (50  $\mu\text{m}$  (i.d.)  $\times$  100 mm) to control the flow rate of gas entering the collision cell. The HCD gas supply line was interrupted by insertion of a 3-way ball valve, which enables switching between the output from the PEEKsil™ restriction and the native nitrogen supply. Downstream from the union tee, ozone is destroyed by a catalytic destruct (IN USA, Norwood, MA) and ultimately exhausted from the laboratory. Ozone monitors (2B Technologies, Boulder, CO) recorded the ozone concentration within the closed system upstream from the union tee and in the ambient laboratory air.

OzID spectra were acquired in a data-independent workflow from  $m/z$  650–950 in 1 Da increments. For these experiments, the mass resolution was set to 240,000 (at  $m/z$  200), the isolation window 1.4 Da, and the collision energy set to the minimum value (10 arbitrary units). Mass-selected precursor ions were exposed to ozone for 0.5 s, preceding mass analysis in the Orbitrap. Ten transients were averaged prior to the Fourier

transform. Post-acquisition, data were visualized and analyzed using Xcalibur Qual Browser (version 3.0.63, Thermo Fisher Scientific). Reconstructed unsaturation profiles from ions exhibiting a common OzID neutral loss were extracted with a tolerance of 0.1 Da.

### Nomenclature

Lipid nomenclature is based on literature recommendations [53, 54]. For example, the shorthand notation PC 34:1 represents a phosphatidylcholine lipid containing 34 carbons and a single double bond within its fatty acyl chains. Unsaturation in a fatty acyl chain is defined with respect to the alkyl terminus by  $(n-x)$ , where  $x$  is the number of carbons from the methyl group to the double bond (e.g., PC 34:1( $n-9$ ))). Note that in this representation, neither the identity of the fatty acid carrying the double bond nor the fatty acid position on the glycerol backbone (*sn*-position) are explicitly identified. When the fatty acid identities are known, the underscore separator is used (e.g., PC 16:0\_18:1( $n-9$ ))). Explicit identification of both the fatty acid identity and *sn*-position is denoted by a slash (e.g., PC 16:0/18:1( $n-9$ ))). Double bond stereochemistry is not explicitly defined.

## Results and Discussion

Previous quantitative studies have determined that the most abundant lipid classes in the plasma lipidome are cholesterol and cholesteryl esters (CE), phosphatidylcholines (PC), phosphatidylethanolamines (PE), triacylglycerols (TG), and sphingomyelin (SM) [9, 14]. Aside from cholesterol, each class is comprised of at least 18 different sum compositions. The aim of the present work is not to recapitulate these studies but to explore the diversity of isomeric structures within a single sum composition assignment. OzID spectra were acquired across the range  $m/z$  650–950 in 1 Da steps for  $[\text{M} + \text{Na}]^+$  ions generated by direct infusion ESI of a plasma lipid extract. The complete dataset (obtained in under 40 min) was subsequently interrogated to explore lipid unsaturation and isomeric diversity in plasma. OzID spectra were obtained for unsaturated lipid species at or above 1 nmol/mL (e.g., Cer d18:1/24:1( $n-9$ )), [9] see Supporting Information Fig. S3).

### Unsaturation in Plasma Cholesteryl Esters

One of the most abundant lipids in human plasma is CE 18:2 (1.8  $\mu\text{mol}/\text{mL}$ ) [9, 14], that is, the cholesteryl ester of a fatty acid with 18 carbons and 2 double bonds. Moreover, CE 18:2 in plasma has been identified as a potential biomarker for squamous cell lung carcinoma [55]. As shown in Fig. 2b, ozonolysis of sodiated CE 18:2 ions ( $m/z$  671.58) in the octopole collision cell for 0.5 s resulted in almost complete reaction of the precursor ion. Ozonolysis yielded an abundant  $[\text{M} + \text{Na} + 16]^+$  product ion ( $m/z$  687.57), assigned to the formation of an epoxide on the tetracyclic sterol ring system [56]. Reaction of the alkene(s) on the fatty acyl chain with ozone can arise

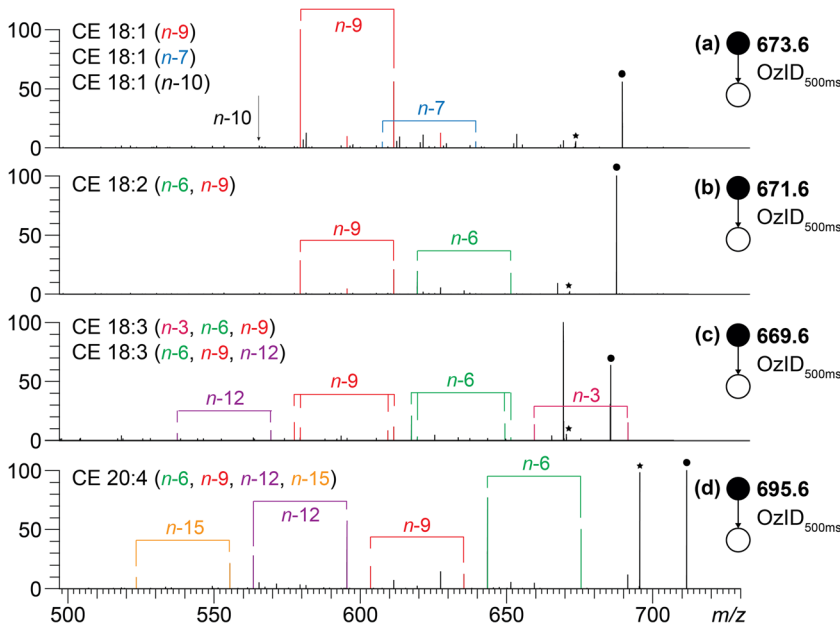


**Figure 2.** OzID spectra obtained for (a) CE 18:1 ( $m/z$  673.59); (b) CE 18:2 ( $m/z$  671.57); (c) CE 18:3 ( $m/z$  669.56); and (d) CE 20:4 ( $m/z$  695.58). The precursor ion in each spectrum is indicated by a star while  $[M + Na + 16]^+$  product ions are denoted by closed circles. OzID product ions indicative of the positions of unsaturation are indicated with colored brackets.

from either the  $[M + Na + 16]^+$  ion or an  $[M + Na + 48]^+$  product ion resulting from ring-opening [56]. As such, 2 pairs of OzID product ions (offset by 32 Da) associated with each double bond of the 18:2 fatty acyl can be assigned according to predictable ozonolysis transitions shown in Tables 1 and 2, consistent with the *n*-6 and *n*-9 double bonds of linoleic acid. Thus the ion at  $m/z$  671.58 can be confidently assigned as exclusively comprising CE 18:2(*n*-6, *n*-9), as reported previously [57]. Similarly, the OzID spectrum in Fig. 2d shows that CE 20:4 ( $m/z$  695.57) is uniquely cholesteryl arachidonate (i.e., CE 20:4(*n*-6, *n*-9, *n*-12, *n*-15)). Conversely, the OzID spectra shown in Fig. 2a and c demonstrate that CE 18:1 ( $m/z$  673.59) and CE 18:3 ( $m/z$  669.56) have contributions from multiple isomers. Neutral losses of 110.15 Da and 94.15 Da (see Table 1) from either the  $[M + Na + 16]^+$  ion or  $[M + Na + 48]^+$  ion indicate that the predominant isomer contributing to  $m/z$  673.59 is CE 18:1(*n*-9). However, aldehyde product ions with a neutral loss of 82.11 Da and 124.16 Da are also observed, at lower abundance, indicative of CE 18:1(*n*-7) and CE 18:1(*n*-10). Differing rates of ozonolysis as a function of double bond position [58] mean that relative quantitation of these

isomers is not possible without reference to pure standards; however, a molar ratio of 1:12 has previously been reported for the CE 18:1(*n*-7) and CE 18:1(*n*-9) isomers, which is consistent with these data [57]. Importantly, although all precursor ions of  $m/z$   $673.6 \pm 0.7$  Da react with ozone in the octopole collision cell in the configuration presented here, subsequent high resolution mass analysis enables the discrimination of isobaric precursor ions (and their reaction products), such that the  $[M + 2]$  isotopic peak of CE 18:2 is resolved from CE 18:1 ( $\Delta = 7.5$  mDa,  $R_s \sim 90,000$ ).

### Trends in Unsaturation Across the Plasma Lipidome

Spectral acquisition in a data-independent workflow enables the compilation of all OzID spectra across the target  $m/z$  range into a heat map, providing a global snapshot of unsaturation in

**Table 2.** Ozonolysis neutral losses (Da) for polyunsaturated FAs

First DB position ( <i>n</i> - <i>x</i> )	All DB positions ( <i>n</i> - <i>x</i> )	Aldehyde	Criegee
3	3	26.0520	10.0571
	6	66.0833	50.0884
	9	106.1146	90.1197
	12	146.1459	130.1510
	15	186.1772	170.1823
	18	226.2085	210.2136
6	6	68.0990	52.1041
	9	108.1303	92.1354
	12	148.1616	132.1667
	15	188.1929	172.1980
	18	228.2242	212.2293
	9	110.1459	94.1510
9	12	150.1772	134.1823
	15	190.2085	174.2136

**Table 1.** Ozonolysis neutral losses (Da) for monounsaturated FAs

DB position ( <i>n</i> - <i>x</i> )	Aldehyde Ion	Criegee Ion
3	26.0520	10.0571
4	40.0677	24.0728
6	68.0990	52.1041
7	82.1146	66.1197
9	110.1459	94.1510
10	124.1616	108.1667
15	194.2398	178.2449
17	222.2711	206.2762

the plasma lipidome. In this representation, as shown in Fig. 3, each vertical slice is an individual OzID spectrum, with all precursor ions falling on a diagonal line. Regardless of their class, all lipid ions with a common position of unsaturation (with respect to the methyl terminus of the fatty acyl) also fall on parallel diagonal lines, as a consequence of the ozonolysis-induced neutral loss.

The data plotted in Fig. 3 can be used to readily identify the major complex lipids containing fatty acyls with a specific position of unsaturation. Integrating along each diagonal line yields a profile of all lipids containing a specific position of unsaturation, in the form of a reconstructed spectrum of all precursor ions exhibiting a common neutral loss, as shown in Fig. 4. For example, the reconstructed neutral loss representation in Fig. 4e shows that the nutritionally essential *n*-3 fatty acyls (identified by a common 26.05 Da loss) are located predominantly in triacylglycerols (TGs) of 50–54 carbons but also identifies PC 36:5 and PC 38:6 as omega-3 fatty acid carriers. Similarly, the profiles of *n*-9, *n*-7, and *n*-6 double bonds (Fig. 4a–c) are also dominated by the highly abundant TGs of 50–52 carbons and, to a lesser extent, PCs of 34–38 carbons. While it must be noted that the ordinate of these reconstructed spectra reflects the raw abundance of OzID product ions (a function of both the precursor ion abundance and ozonolysis reaction rate), these reconstructed neutral loss spectra afford a rich, qualitative snapshot of unsaturation across the extract.

Compared with C=C double bonds within fatty acyl chains, the *trans* *n*-14 double bond within a sphingolipid long-chain base is relatively unreactive toward ozone. [59] Thus, a neutral loss of 180.22 Da, diagnostic for an *n*-14 alkene, does not yield a useful profile of sphingosine-containing lipids. As shown in Fig. 4d however, a neutral loss of 40.07 Da during ozonolysis (indicative of an *n*-4 double bond) is exclusive to sphingomyelins with at least 2 sites of unsaturation. This hypothesis is consistent with the presence of an (*n*-4, *n*-14)-

sphingadiene as the long-chain sphingoid base, [60] although it is feasible that the *n*-4 double bond may instead be on the fatty acyl. For example, SM d34:2 in human plasma consists of 85% SM d18:2/16:0, whereas only 29% of SM d42:2 carries a sphingadiene motif, as determined by MS/MS in negative ion mode [9]. The OzID spectrum acquired from the [SM d34:2 + Na]<sup>+</sup> ion (*m/z* 723.54) features abundant product ions assigned to the *n*-4 double bond position. By contrast, ozonolysis of SM d42:2 (*m/z* 835.67) yields product ions diagnostic for both the *n*-4 and *n*-9 positions. The abundance of the latter ions are greater than the former, consistent with the presence of SM d18:1/24:1(*n*-9) as the major isomer, and SM d18:2(*n*-4, *n*-14)/24:0 as the minor contributor (see Supporting Information, Fig. S4).

### High Resolution MS with OzID Resolves Isobaric and Isomeric Lipids

Plasmanyl-, and plasmenyl- (i.e., plasmalogen) ether lipids are isomeric species that are not typically resolved by chromatography or low-energy CID, although selective chemical derivatization of the plasmalogen double bond has proven successful [61]. Previous studies of human plasma have grouped isomeric alkyl ether and vinyl ether lipids (with the same total number of double bonds) together as single species [9]. Plasmalogens are differentiated from their alkyl ether counterparts by the rapid reaction of the electron-rich vinyl ether with ozone, resulting in a neutral loss of 194.24 Da (for *P*-16:0) or 222.27 Da (for *P*-18:0). [62] Fig. 5 highlights that the major PC plasmalogens in human plasma contain 32–38 carbons, generally partnered by a polyunsaturated fatty acid (PUFA). For example, the largest peak identified for both *P*-16:0 (Fig. 5a) and *P*-18:0 (Fig. 5b) species contains a 20:4 fatty acid. Note that the relative abundances obtained from these profiles differ from the total ether PC lipid profile previously reported [9, 14]. These data confirm that plasmalogens exhibit a unique profile that is concealed in

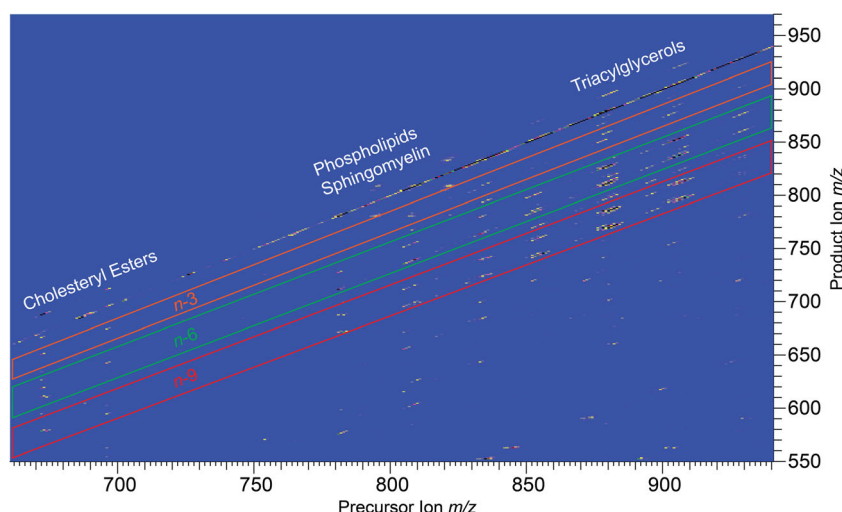


**Figure 3.** The unsaturation profile of complex plasma lipids from a data-independent OzID workflow obtained by plotting all precursor ions against product ions. Ions corresponding to all lipid carriers of *n*-6 and *n*-9 double bonds are indicated by highlighted diagonal lines

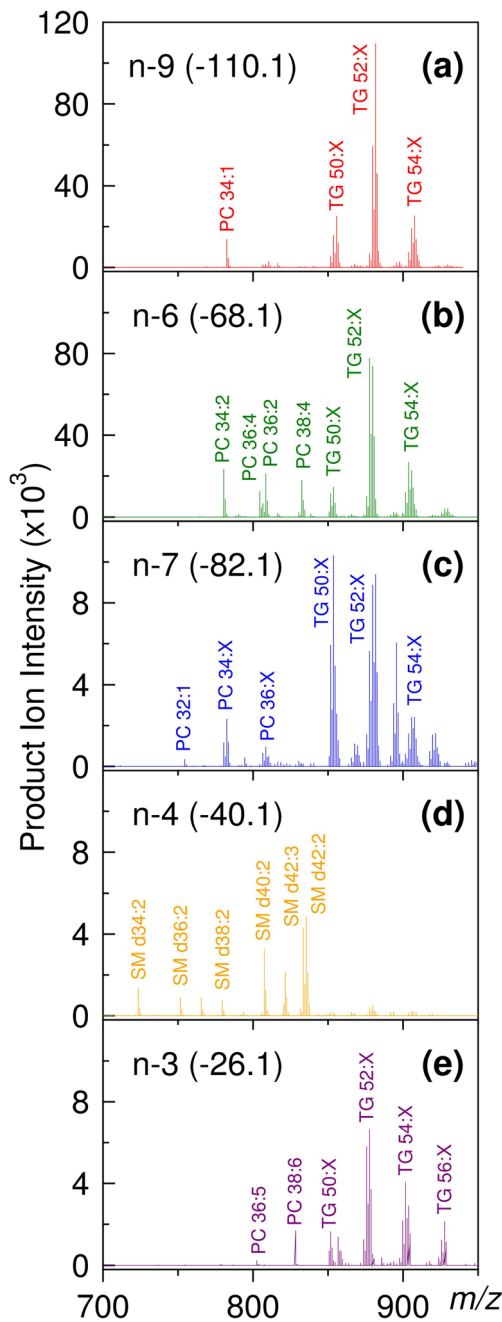


**Figure 4.** Unsaturation profiles reconstructed from ions exhibiting a common neutral loss (indicated in parentheses). Cholesterol esters are not shown in these profiles due to additional reaction of the sterol head group with ozone

measurements that do not resolve these species from isomeric plasmanyl alkyl ether lipids. Moreover, from these data, it is clear that biomarkers identified only at the sum composition level can actually be isomeric mixtures. For example, plasma PC O-38:5 has been proposed as a plasma biomarker for prostate cancer [3] but is in fact comprised of at least 4 isomers (see Supporting Information, Fig. S5).

High-resolution mass analysers are beneficial for resolving isobaric lipid ions in complex samples [63]. Highlighting the utility of applying OzID on an Orbitrap

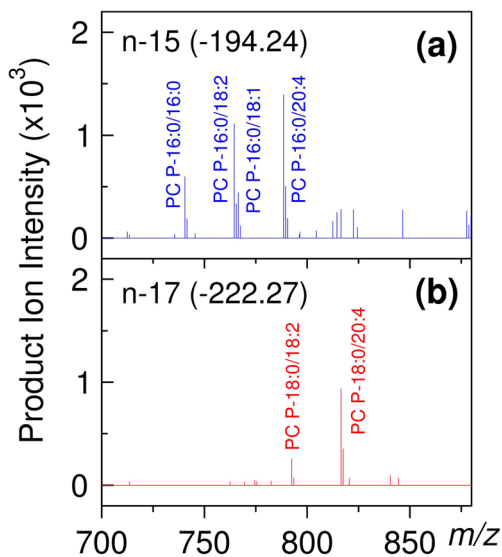


**Figure 5.** Compiling all precursor ions exhibiting a common neutral loss characteristic for: (a) n-15 or (b) n-17 double bonds generates a profile of all plasmalogens

mass spectrometer, ether-linked PCs are differentiated from isobaric dialkyl PEs (with 2 additional carbons in the fatty acyls) that differ in mass by approximately 38 mDa ( $R_s \sim 20,000$ ). As the neutral loss is consistent for all double bonds at the same ( $n$ - $x$ ) position, it follows that product ions resulting from ozonolysis will be similarly resolved. The OzID spectrum shown in Fig. 6 demonstrates that both PC O-34:1 ( $m/z$  768.59) and PE 36:1 ( $m/z$  768.55) carry n-9 double bonds. Moreover, the absence of product ions corresponding to n-15 or n-17 double bonds (see Fig. 5) confirms that PC O-34:1 is

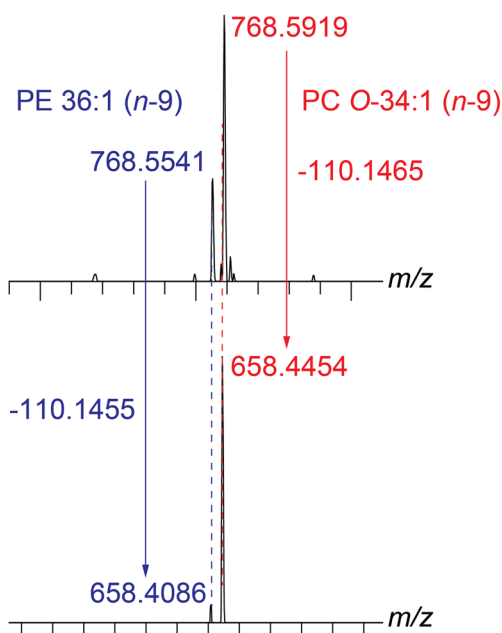


**Figure 6.** Identification of n-9 double bonds in isobaric PC O-34:1 and PE 36:1 lipids

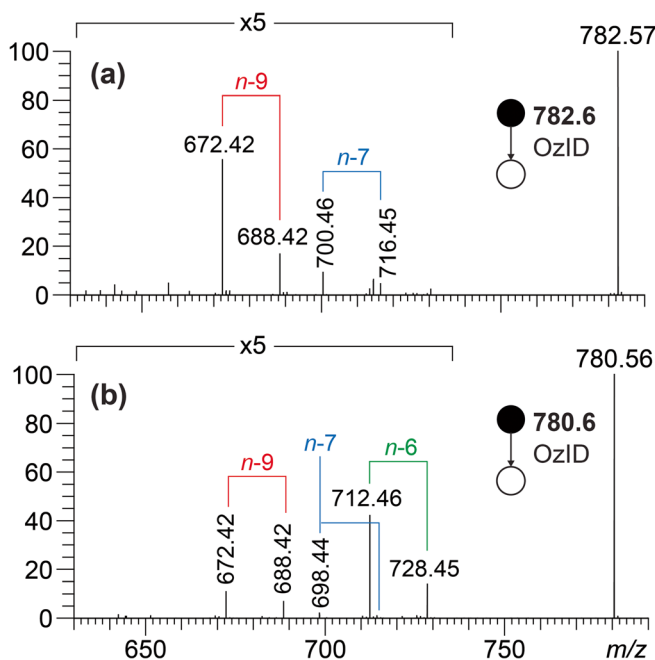


**Figure 7.** Ozone induced-dissociation mass spectra obtained for (a) PC 34:1 ( $m/z$  782.57); (b) PC 34:2 ( $m/z$  780.57). Ozonolysis of phosphatidylcholines identifies multiple double bond isomers but does not pinpoint the fatty acyl moiety on which they are located

comprised exclusively of plasmanyl ether lipids, and plasmalogens are not present.

#### Towards Identification of Structurally-Defined Lipids

Based on these data alone, it must be emphasized that the position of unsaturation cannot be localized to a specific fatty acyl moiety within a complex lipid. For example, identification of an *n*-9 double bond from ozonolysis of PC 34:1 is insufficient to distinguish isomers that vary in the composition of fatty acyl chains (e.g., PC 16:0/18:1(*n*-9), PC 18:0/16:1(*n*-9)) and relative *sn*-position (e.g., PC 18:1(*n*-9)/16:0, PC 16:0/18:1(*n*-9)). As demonstrated above for sphingomyelins, further insight can be obtained by combining DIA-OzID data with results from MS/MS experiments that resolve such ambiguities. For example, the major isomer of PC 34:1 in human plasma is PC 16:0/18:1 (89%), followed by the alternate regioisomer PC 18:1/16:0 (11%) [30]. As shown in Fig. 7a, ozonolysis of sodiated PC 34:1 ions ( $m/z$  782.57) yields pairs of product ions assigned to the *n*-9 (major) or *n*-7 (minor) double bonds of a monounsaturated fatty acid. In the absence of PC 18:0\_16:1 or other fatty acid combinations, these double bonds can be uniquely assigned to 2 different isomers of an 18:1 fatty acyl. Comprising 2 different regioisomers and 2 double bond positions, PC 34:1 is composed of up to 4 distinct isomers, namely PC 16:0/18:1(*n*-7), PC 16:0/18:1(*n*-9), PC 18:1(*n*-7)/16:0, and/or PC 18:1(*n*-9)/16:0, consistent with recent analysis by Zhang and co-workers [48]. Further MS<sup>n</sup> interrogation

of the precursor ion using a top-down combination of CID and OzID on an ion trap mass spectrometer would be required to determine whether a specific double bond position is selectively partitioned to the 18:1 fatty acyl at the *sn*-1 or *sn*-2 position, and unambiguously assign the lipid structure [25]. Similarly, PC 34:2 in human plasma is comprised of predominantly PC 16:0/18:2 and its regioisomer PC 18:2/16:0 [30]. As shown in Fig. 7b, the OzID spectrum of PC 34:2 features pairs of product ions assigned to the *n*-6 and *n*-9 double bonds of a PUFA, consistent with linoleic acid. Also observed in the OzID spectrum are product ions assigned to a mono-unsaturated FA with a double bond in either the *n*-7 and *n*-9 position, consistent with the presence of PC 16:1\_18:1 in human plasma [48, 64].

#### Conclusions

The array of lipids found in human plasma is remarkably diverse in terms of structure and concentration, posing a significant analytical challenge to the complete quantitative elucidation of the lipidome. Even with the additional dimension of MS/MS, most mass spectrometry-based methods identify plasma lipids only at the sum composition or molecular lipid level, thus the complexity of the plasma lipidome is systematically understated. In this work, ozonolysis was implemented as part of a data-independent acquisition workflow on a high-resolution mass spectrometer in order to resolve this complication by profiling unsaturation in human plasma lipids across a wide dynamic range down to the low nmol/mL level. Regardless of lipid class, fatty acyls with a common position of unsaturation relative to the methyl terminus can be classified by a characteristic neutral loss resulting from ozonolysis of the alkene. This enables the post-acquisition generation of pseudo neutral loss profiles for a given double bond position in monounsaturated and polyunsaturated lipids. Using this approach, plasmalogens are readily distinguished from isomeric plasmanyl ether lipids and isobaric interferences by the presence of the vinyl ether double bond.

Qualitatively, the predominant double bond positions within fatty acyls are consistent across the major lipid classes. Previous studies have shown that the distribution of carbon-carbon double bond locations within fatty acyl chains are tightly conserved between free fatty acids and cholesterol esters within a common plasma sample [47, 57]. The conservation of double bond profile between different lipid classes confirms their common origins in lipid biosynthesis. More broadly, the data obtained here represent a comprehensive archive of unsaturation in the human plasma lipidome and will be a valuable resource to interrogate for unresolved isomers as new lipid biomarkers are identified. Moreover, this profile may be used to identify target lipids for comprehensive structural analysis using complementary MS<sup>n</sup> methods [25].

## Acknowledgements

The authors acknowledge generous financial support provided by the Australian Research Council (ARC) through the Discovery Program (DP150101715 and DP190101486), and the EU H2020 funded MASSTRPLAN project (grant number 675132). Some of the data reported here were acquired at the QUT Central Analytical Research Facility (CARF) operated by the Institute for Future Environments.

## Data Availability

A comparison of OzID efficiency in an octopole collision cell and a linear ion trap is included as Supporting Information, alongside example OzID spectra for Cer d42:2, SM d34:2, SM d42:2, and PC O-38:5. An archive of OzID spectral data acquired in this study is freely available at <https://doi.org/10.25912/5ca3eed161916>.

## References

- Quehenberger, O., Dennis, E.A.: The human plasma lipidome. *N Engl. J. Med.* **365**, 1812–1823 (2011)
- Mapstone, M., Cheema, A.K., Fiandaca, M.S., Zhong, X., Mhyre, T.R., MacArthur, L.H., Hall, W.J., Fisher, S.G., Peterson, D.R., Haley, J.M., Nazar, M.D., Rich, S.A., Berlau, D.J., Peltz, C.B., Tan, M.T., Kawas, C.H., Federoff, H.J.: Plasma phospholipids identify antecedent memory impairment in older adults. *Nat. Med.* **20**, 415–418 (2014)
- Lin, H.-M., Mahon, K.L., Weir, J.M., Mundra, P.A., Spielman, C., Briscoe, K., Gurney, H., Mallesara, G., Marx, G., Stockler, M.R., Consortium, P., Parton, R.G., Hoy, A.J., Daly, R.J., Meikle, P.J., Horvath, L.G.: A distinct plasma lipid signature associated with poor prognosis in castration-resistant prostate cancer. *Int. J. Cancer.* **141**, 2112–2120 (2017)
- Mousa, A., Naderpoor, N., Mellett, N., Wilson, K., Plebanski, M., Meikle, P.J., de Courten, B.: Lipidomic profiling reveals early-stage metabolic dysfunction in overweight or obese humans. *Biochim. Biophys. Acta Mol. Cell Biol. Lipids.* **1864**, 335–343 (2019)
- Mundra, P.A., Barlow, C.K., Nestel, P.J., Barnes, E.H., Kirby, A., Thompson, P., Sullivan, D.R., Alshehry, Z.H., Mellett, N.A., Huynh, K., Jayawardana, K.S., Giles, C., McConville, M.J., Zoungas, S., Hillis, G.S., Chalmers, J., Woodward, M., Wong, G., Kingwell, B.A., Simes, J., Tonkin, A.M., Meikle, P.J., Investigators, L.S.: Large-scale plasma lipidomic profiling identifies lipids that predict cardiovascular events in secondary prevention. *JCI Insight.* **3**, e121326 (2018)
- Vvedenskaya, O., Wang, Y., Ackerman, J.M., Knittelfelder, O., Shevchenko, A.: Analytical challenges in human plasma lipidomics: a winding path towards the truth. *TrAC Trends Anal. Chem.* (2018) <https://doi.org/10.1016/j.trac.2018.10.013>
- Schuhmann, K., Almeida, R., Baumert, M., Herzog, R., Bornstein, S.R., Shevchenko, A.: Shotgun lipidomics on a LTQ Orbitrap mass spectrometer by successive switching between acquisition polarity modes. *J. Mass Spectrom.* **47**, 96–104 (2012)
- Gallego, S.F., Hojlund, K., Ejsing, C.S.: Easy, fast, and reproducible quantification of cholesterol and other lipids in human plasma by combined high resolution MSX and FTMS analysis. *J. Am. Soc. Mass Spectrom.* **29**, 34–41 (2018)
- Quehenberger, O., Armando, A.M., Brown, A.H., Milne, S.B., Myers, D.S., Merrill, A.H., Bandyopadhyay, S., Jones, K.N., Kelly, S., Shaner, R.L., Sullards, C.M., Wang, E., Murphy, R.C., Barkley, R.M., Leiker, T.J., Raetz, C.R.H., Guan, Z., Laird, G.M., Six, D.A., Russell, D.W., McDonald, J.G., Subramaniam, S., Fahy, E., Dennis, E.A.: Lipidomics reveals a remarkable diversity of lipids in human plasma. *J. Lipid Res.* **51**, 3299–3305 (2010)
- Baglai, A., Gargano, A.F.G., Jordens, J., Mengerink, Y., Honing, M., van der Wal, S., Schoenmakers, P.J.: Comprehensive lipidomic analysis of human plasma using multidimensional liquid- and gas-phase separations: two-dimensional liquid chromatography–mass spectrometry vs. liquid chromatography–trapped-ion-mobility–mass spectrometry. *J. Chromatogr. A.* **1530**, 90–103 (2017)
- Rampler, E., Criscuolo, A., Zeller, M., El Abied, Y., Schoeny, H., Hermann, G., Sokol, E., Cook, K., Peake, D.A., Delanghe, B., Koellensperger, G.: A novel Lipidomics workflow for improved human plasma identification and quantification using RPLC-MSn methods and isotope dilution strategies. *Anal. Chem.* **90**, 6494–6501 (2018)
- Christinat, N., Morin-Rivron, D., Masoodi, M.: High-throughput quantitative lipidomics analysis of nonesterified fatty acids in human plasma. *J. Proteome Res.* **15**, 2228–2235 (2016)
- Phinney, K.W., Ballihaut, G., Bedner, M., Benford, B.S., Camara, J.E., Christopher, S.J., Davis, W.C., Dodder, N.G., Eppe, G., Lang, B.E., Long, S.E., Lowenthal, M.S., McGaw, E.A., Murphy, K.E., Nelson, B.C., Prendergast, J.L., Reiner, J.L., Rimmer, C.A., Sander, L.C., Schantz, M.M., Sharpless, K.E., Sniegowski, L.T., Tai, S.S.C., Thomas, J.B., Vetter, T.W., Welch, M.J., Wise, S.A., Wood, L.J., Guthrie, W.F., Hagwood, C.R., Leigh, S.D., Yen, J.H., Zhang, N.-F., Chaudhary-Webb, M., Chen, H., Fazili, Z., LaVoie, D.J., McCoy, L.F., Momin, S.S., Paladugula, N., Pendergrast, E.C., Pfeiffer, C.M., Powers, C.D., Rabinowitz, D., Rybak, M.E., Schleicher, R.L., Toombs, B.M.H., Xu, M., Zhang, M., Castle, A.L.: Development of a standard reference material for metabolomics research. *Anal. Chem.* **85**, 11732–11738 (2013)
- Bowden, J.A., Heckert, A., Ulmer, C.Z., Jones, C.M., Koelmel, J.P., Abdullah, L., Ahonen, L., Alnouti, Y., Armando, A.M., Asara, J.M., Bamba, T., Barr, J.R., Bergquist, J., Borchers, C.H., Brandsma, J., Breitkopf, S.B., Cajka, T., Cazenave-Gassiot, A., Checa, A., Cinel, M.A., Colas, R.A., Cremers, S., Dennis, E.A., Evans, J.E., Fauland, A., Fiehn, O., Gardner, M.S., Garrett, T.J., Gotlinger, K.H., Han, J., Huang, Y., Neo, A.H., Hyötyläinen, T., Izumi, Y., Jiang, H., Jiang, H., Jiang, J., Kachman, M., Kiyonami, R., Klavins, K., Klose, C., Köfeler, H.C., Kolmert, J., Koal, T., Koster, G., Kuklenyik, Z., Kurland, I.J., Leadley, M., Lin, K., Maddipati, K.R., McDougall, D., Meikle, P.J., Mellett, N.A., Monnin, C., Moseley, M.A., Nandakumar, R., Oresic, M., Patterson, R., Peake, D., Pierce, J.S., Post, M., Postle, A.D., Pugh, R., Qiu, Y., Quehenberger, O., Ramrup, P., Rees, J., Rembiesa, B., Reynaud, D., Roth, M.R., Sales, S., Schuhmann, K., Schwartzman, M.L., Serhan, C.N., Shevchenko, A., Somerville, S.E., St. John Williams, L., Surma, M.A., Takeda, H., Thakare, R., Thompson, J.W., Torta, F., Triebel, A., Trötzmüller, M., Ubhayasekera, S.J.K., Vuckovic, D., Weir, J.M., Welti, R., Wenk, M.R., Wheelock, C.E., Yao, L., Yuan, M., Zhao, X.H., Zhou, S.: Harmonizing lipidomics: NIST interlaboratory comparison exercise for lipidomics using SRM 1950–metabolites in frozen human plasma. *J. Lipid Res.* **58**, 2275–2288 (2017)
- Burla, B., Arita, M., Arita, M., Bendt, A.K., Cazenave-Gassiot, A., Dennis, E.A., Ekorroos, K., Han, X., Ikeda, K., Liebisch, G., Lin, M.K., Loh, T.P., Meikle, P.J., Orešić, M., Quehenberger, O., Shevchenko, A., Torta, F., Wakelam, M.J.O., Wheelock, C.E., Wenk, M.R.: MS-based lipidomics of human blood plasma: a community-initiated position paper to develop accepted guidelines. *J. Lipid Res.* **59**, 2001–2017 (2018)
- Bowden, J.A., Ulmer, C.Z., Jones, C.M., Koelmel, J.P., Yost, R.A.: NIST lipidomics workflow questionnaire: an assessment of community-wide methodologies and perspectives. *Metabolomics.* **14**(53), (2018)
- Liebisch, G., Ekorroos, K., Hermansson, M., Ejsing, C.S.: Reporting of lipidomics data should be standardized. *Biochim. Biophys. Acta Mol. Cell Biol. Lipids.* **1862**, 747–751 (2017)
- Koelmel, J.P., Ulmer, C.Z., Jones, C.M., Yost, R.A., Bowden, J.A.: Common cases of improper lipid annotation using high-resolution tandem mass spectrometry data and corresponding limitations in biological interpretation. *Biochim. Biophys. Acta Mol. Cell Biol. Lipids.* **1862**, 766–770 (2017)
- Hancock, S.E., Poole, B.L.J., Batarseh, A., Abbott, S.K., Mitchell, T.W.: Advances and unresolved challenges in the structural characterization of isomeric lipids. *Anal. Biochem.* **524**, 45–55 (2017)
- Shevchenko, A., Simons, K.: Lipidomics: coming to grips with lipid diversity. *Nat. Rev. Mol. Cell Biol.* **11**, 593–598 (2010)
- Wozny, K., Lehmann, W.D., Wozny, M., Akbulut, B.S., Brügger, B.: A method for the quantitative determination of glycerophospholipid regioisomers by UPLC-ESI-MS/MS. *Anal. Bioanal. Chem.* **411**, 915–924 (2019)
- Kozlowski, R.L., Mitchell, T.W., Blanksby, S.J.: Separation and identification of phosphatidylcholine regioisomers by combining liquid chromatography with a fusion of collision-and ozone-induced dissociation. *Eur. J. Mass Spectrom.* **21**, 191–200 (2015)

23. Maccarone, A.T., Duldig, J., Mitchell, T.W., Blanksby, S.J., Duchoslav, E., Campbell, J.L.: Characterization of acyl chain position in unsaturated phosphatidylcholines using differential mobility-mass spectrometry. *J. Lipid Res.* **55**, 1668–1677 (2014)
24. Marshall, D.L., Pham, H.T., Bhujel, M., Chin, J.S.R., Yew, J.Y., Mori, K., Mitchell, T.W., Blanksby, S.J.: Sequential collision- and ozone-induced dissociation enables assignment of relative acyl chain position in triacylglycerols. *Anal. Chem.* **88**, 2685–2692 (2016)
25. Pham, H.T., Maccarone, A.T., Thomas, M.C., Campbell, J.L., Mitchell, T.W., Blanksby, S.J.: Structural characterization of glycerophospholipids by combinations of ozone- and collision-induced dissociation mass spectrometry: the next step towards "top-down" lipidomics. *Analyst* **139**, 204–214 (2014)
26. Leskinen, H.M., Suomela, J.-P., Kallio, H.P.: Quantification of triacylglycerol regiosomers by ultra-high-performance liquid chromatography and ammonia negative ion atmospheric pressure chemical ionization tandem mass spectrometry. *Rapid Commun. Mass Spectrom.* **24**, 1–5 (2010)
27. Řezánka, T., Pádrová, K., Sigler, K.: Regioisomeric and enantiomeric analysis of triacylglycerols. *Anal. Biochem.* **524**, 3–12 (2017)
28. Ekroos, K., Ejsing, C.S., Bahr, U., Karas, M., Simons, K., Shevchenko, A.: Charting molecular composition of phosphatidylcholines by fatty acid scanning and ion trap MS3 fragmentation. *J. Lipid Res.* **44**, 2181–2192 (2003)
29. Han, X., Gross, R.W.: Structural determination of picomole amounts of phospholipids via electrospray ionization tandem mass spectrometry. *J. Am. Soc. Mass Spectrom.* **6**, 1202–1210 (1995)
30. Zacek, P., Bukowski, M., Rosenberger, T.A., Picklo, M.: Quantitation of isobaric phosphatidylcholine species in human plasma using a hybrid quadrupole linear ion-trap mass spectrometer. *J. Lipid Res.* **57**, 2225–2234 (2016)
31. Ekroos, K.: Lipidomics perspective: from molecular lipidomics to validated clinical diagnostics. In: Ekroos, K. (ed.). Wiley-VCH, Weinheim (2012)
32. Martínez-Seara, H., Róig, T., Pasenkiewicz-Gierula, M., Vattulainen, I., Karttunen, M., Reigada, R.: Effect of double bond position on lipid bilayer properties: insight through atomistic simulations. *J. Phys. Chem. B* **111**, 11162–11168 (2007)
33. Martínez-Seara, H., Róig, T., Pasenkiewicz-Gierula, M., Vattulainen, I., Karttunen, M., Reigada, R.: Interplay of unsaturated phospholipids and cholesterol in membranes: effect of the double-bond position. *Biophys. J.* **95**, 3295–3305 (2008)
34. Renne, M.F., de Kroon, A.I.P.M.: The role of phospholipid molecular species in determining the physical properties of yeast membranes. *FEBS Lett.* **592**, 1330–1345 (2018)
35. Ma, X., Chong, L., Tian, R., Shi, R., Hu, T.Y., Ouyang, Z., Xia, Y.: Identification and quantitation of lipid C=C location isomers: a shotgun lipidomics approach enabled by photochemical reaction. *Proc. Natl. Acad. Sci. U. S. A.* **113**, 2573–2578 (2016)
36. Vriens, K., Christen, S., Parik, S., Broekaert, D., Yoshinaga, K., Talebi, A., Dehairs, J., Escalona-Noguero, C., Schmieder, R., Cornfield, T., Charlton, C., Romero-Pérez, L., Rossi, M., Rinaldi, G., Orth, M.F., Boon, R., Kerstens, A., Kwan, S.Y., Faubert, B., Méndez-Lucas, A., Kopitz, C.C., Chen, T., Fernandez-Garcia, J., Duarte, J.A.G., Schmitz, A.A., Steigemann, P., Najimi, M., Hägebarth, A., Van Ginderachter, J.A., Sokal, E., Gotoh, N., Wong, K.-K., Verfaillie, C., Derua, R., Munck, S., Yuneva, M., Beretta, L., DeBerardinis, R.J., Swinnen, J.V., Hodson, L., Cassiman, D., Verslype, C., Christian, S., Grünewald, S., Grünewald, T.G.P., Fendt, S.-M.: Evidence for an alternative fatty acid desaturation pathway increasing cancer plasticity. *Nature* **566**, 403–406 (2019)
37. Pauling, J.K., Hermansson, M., Hartler, J., Christiansen, K., Gallego, S.F., Peng, B., Ahrends, R., Ejsing, C.S.: Proposal for a common nomenclature for fragment ions in mass spectra of lipids. *PLoS One* **12**, e0188394 (2017)
38. Poad, B.L.J., Maccarone, A.T., Yu, H., Mitchell, T.W., Saied, E.M., Arenz, C., Hornemann, T., Bull, J.N., Bieske, E.J., Blanksby, S.J.: Differential-mobility spectrometry of 1-deoxysphingosine isomers: new insights into the gas phase structures of ionized lipids. *Anal. Chem.* **90**, 5343–5351 (2018)
39. Groessl, M., Graf, S., Knochenmuss, R.: High resolution ion mobility-mass spectrometry for separation and identification of isomeric lipids. *Analyst* **140**, 6904–6911 (2015)
40. Kyle, J.E., Zhang, X., Weitz, K.K., Monroe, M.E., Ibrahim, Y.M., Moore, R.J., Cha, J., Sun, X., Lovelace, E.S., Wagoner, J., Polyak, S.J., Metz, T.O., Dey, S.K., Smith, R.D., Burnum-Johnson, K.E., Baker, E.S.: Uncovering biologically significant lipid isomers with liquid chromatography, ion mobility spectrometry and mass spectrometry. *Analyst* **141**, 1649–1659 (2016)
41. Ma, X., Xia, Y.: Pinpointing double bonds in lipids by Paternò-Büchi reactions and mass spectrometry. *Angew. Chem. Int. Ed.* **53**, 2592–2596 (2014)
42. Ryan, E., Nguyen, C.Q.N., Shiea, C., Reid, G.E.: Detailed structural characterization of sphingolipids via 193 nm ultraviolet photodissociation and ultra high resolution tandem mass spectrometry. *J. Am. Soc. Mass Spectrom.* **28**, 1406–1419 (2017)
43. Williams, P.E., Klein, D.R., Greer, S.M., Brodbelt, J.S.: Pinpointing double bond and sn-positions in glycerophospholipids via hybrid 193 nm ultraviolet photodissociation (UVPD) mass spectrometry. *J. Am. Chem. Soc.* **139**, 15681–15690 (2017)
44. Campbell, J.L., Baba, T.: Near-complete structural characterization of phosphatidylcholines using electron impact excitation of ions from organics. *Anal. Chem.* **87**, 5837–5845 (2015)
45. Yang, K., Dilthey, B.G., Gross, R.W.: Identification and quantitation of fatty acid double bond positional isomers: a shotgun lipidomics approach using charge-switch derivatization. *Anal. Chem.* **85**, 9742–9750 (2013)
46. Wang, M., Han, R.H., Han, X.: Fatty acidomics: global analysis of lipid species containing a carboxyl group with a charge-remote fragmentation-assisted approach. *Anal. Chem.* **85**, 9312–9320 (2013)
47. Ma, X., Zhao, X., Li, J., Zhang, W., Cheng, J.-X., Ouyang, Z., Xia, Y.: Photochemical tagging for quantitation of unsaturated fatty acids by mass spectrometry. *Anal. Chem.* **88**, 8931–8935 (2016)
48. Zhang, W.P., Zhang, D.H., Chen, Q.H., Wu, J.H., Ouyang, Z., Xia, Y.: Online photochemical derivatization enables comprehensive mass spectrometric analysis of unsaturated phospholipid isomers. *Nat. Commun.* **10**, 79 (2019)
49. Thomas, M.C., Mitchell, T.W., Blanksby, S.J.: Online ozonolysis methods for the determination of double bond position in unsaturated lipids. *Methods Mol. Biol.* **579**, 413–441 (2009)
50. Thomas, M.C., Mitchell, T.W., Harman, D.G., Deeley, J.M., Nealon, J.R., Blanksby, S.J.: Ozone-induced dissociation: elucidation of double bond position within mass-selected lipid ions. *Anal. Chem.* **80**, 303–311 (2008)
51. Matyash, V., Liebisch, G., Kurzhalia, T.V., Shevchenko, A., Schwudke, D.: Lipid extraction by methyl-tert-butyl ether for high-throughput lipidomics. *J. Lipid Res.* **49**, 1137–1146 (2008)
52. Olsen, J.V., Macek, B., Lange, O., Makarov, A., Horning, S., Mann, M.: Higher-energy C-trap dissociation for peptide modification analysis. *Nat. Methods* **4**, 709–712 (2007)
53. Liebisch, G., Vizcaíno, J.A., Köfeler, H., Trötzmüller, M., Griffiths, W.J., Schmitz, G., Spener, F., Wakelam, M.J.O.: Shorthand notation for lipid structures derived from mass spectrometry. *J. Lipid Res.* **54**, 1523–1530 (2013)
54. Fahy, E., Subramaniam, S., Brown, H.A., Glass, C.K., Merrill, A.H., Murphy, R.C., Raetz, C.R.H., Russell, D.W., Seyama, Y., Shaw, W., Shimizu, T., Spener, F., van Meer, G., VanNieuwenhze, M.S., White, S.H., Witztum, J.L., Dennis, E.A.: A comprehensive classification system for lipids. *J. Lipid Res.* **46**, 839–862 (2005)
55. Yu, Z., Chen, H., Zhu, Y., Ai, J., Li, Y., Gu, W., Borgia, J.A., Zhang, J., Jiang, B., Chen, W., Deng, Y.: Global lipidomics reveals two plasma lipids as novel biomarkers for the detection of squamous cell lung cancer: a pilot study. *Oncol. Lett.* **16**(761–768), (2018)
56. Hancock, S.E., Maccarone, A.T., Poad, B.L.J., Trevitt, A.J., Mitchell, T.W., Blanksby, S.J.: Reaction of ionised sterol esters with ozone in the gas phase. *Chem. Phys. Lipids* **221**, 198–206 (2019)
57. Ren, J., Franklin, E.T., Xia, Y.: Uncovering structural diversity of unsaturated fatty acyls in cholesteryl esters via photochemical reaction and tandem mass spectrometry. *J. Am. Soc. Mass Spectrom.* **28**, 1432–1441 (2017)
58. Poad, B.L.J., Pham, H.T., Thomas, M.C., Nealon, J.R., Campbell, J.L., Mitchell, T.W., Blanksby, S.J.: Ozone-induced dissociation on a modified tandem linear ion-trap: observations of different reactivity for isomeric lipids. *J. Am. Soc. Mass Spectrom.* **21**, 1989–1999 (2010)
59. Barrientos, R.C., Vu, N., Zhang, Q.: Structural analysis of unsaturated glycosphingolipids using shotgun ozone-induced dissociation mass spectrometry. *J. Am. Soc. Mass Spectrom.* **28**, 2330–2343 (2017)
60. Steiner, R., Saied, E.M., Othman, A., Arenz, C., Maccarone, A.T., Poad, B.L.J., Blanksby, S.J., von Eckardstein, A., Hornemann, T.: Elucidating

- the chemical structure of native 1-deoxysphingosine. *J. Lipid Res.* **57**, 1194–1203 (2016)
- 61. Ryan, E., Reid, G.E.: Chemical derivatization and ultrahigh resolution and accurate mass spectrometry strategies for “shotgun” lipidome analysis. *Acc. Chem. Res.* **49**, 1596–1604 (2016)
  - 62. Thomas, M.C., Mitchell, T.W., Harman, D.G., Deeley, J.M., Murphy, R.C., Blanksby, S.J.: Elucidation of double bond position in unsaturated lipids by ozone electrospray ionization mass spectrometry. *Anal. Chem.* **79**, 5013–5022 (2007)
  - 63. Bielow, C., Mastrobuoni, G., Orioli, M., Kempa, S.: On mass ambiguities in high-resolution shotgun lipidomics. *Anal. Chem.* **89**, 2986–2994 (2017)
  - 64. Heiskanen, L.A., Suoniemi, M., Ta, H.X., Tarasov, K., Ekroos, K.: Long-term performance and stability of molecular shotgun lipidomic analysis of human plasma samples. *Anal. Chem.* **85**, 8757–8763 (2013)